Soil & Tillage Research 186 (2019) 310–321

Contents lists available at ScienceDirect

Soil & Tillage Research

journal homepage: www.elsevier.com/locate/still

# Environmental controls and long-term changes on carbon stocks under agricultural lands

Paulina B. Ramírez[a], Francisco J. Calderón[b], Steven J. Fonte[c], Carlos A. Bonilla[a,d,*]

[a] Departamento de Ingeniería Hidráulica y Ambiental, Pontificia Universidad Católica de Chile, Av. Vicuña Mackenna, 4860, Macul, Santiago, 7820436, Chile
[b] Central Great Plains Research Station, USDA–ARS Akron, CO, 80720, USA
[c] Department of Soil and Crop Sciences, Colorado State University, Fort Collins, CO, 80523, USA
[d] Centro de Desarrollo Urbano Sustentable CONICYT/FONDAP/15110020, El Comendador 1916, Providencia, Santiago, 7520245, Chile

ARTICLE INFO

*Keywords:*
Mid-infrared spectroscopy
Mollisols
Near-infrared spectroscopy
Phyllosilicate clay
Soil carbon sequestration

ABSTRACT

Improved understanding of changes in soil organic carbon (SOC) stocks is critical for developing strategies that ensure effective climate change mitigation and the long-term productivity. Changes in SOC are likely to vary across soil and climate conditions, yet long-term data to elucidate these trends across different ecosystems remains limited. In this study we evaluated long-term changes in SOC across a gradient of climate conditions (from arid to hyper humid), soil orders, and land uses (non- cultivated, woody perennial, and cultivated) in central Chile. Thus, we sought to find evidence for SOC changes in the agricultural lands over past three or four decades. Surface soils (8–29 cm depth) were sampled between 2014 and 2016 and analyzed for total C and N content, aggregate stability, texture, bulk density, pH as well as spectral properties using Mid-infrared (MidIR) and Near-infrared spectroscopy. SOC stocks were compared to those previously measured at the same sites between 1968 and 1994, covering a wide range of SOC values (from 12 Mg C $ha^{-1}$ to 128 Mg C $ha^{-1}$). Our findings show that the largest SOC losses occurred in semiarid and subhumid areas for the time frame considered, decreasing from their initial C stocks by 24.7% and 26.1%, respectively. Moreover, cultivated soils in semiarid regions were more vulnerable than those in arid regions to SOC losses. The results also indicated that in cooler and humid regions, SOC stocks were stable or increased over time. Among soil orders, Mollisols showed the largest losses (29.9% reduction between sampling dates). The MidIR results indicate that the mineral bands for clays and silicates were associated with these sites demonstrating SOC conservation, suggesting that mineral protection played an important role in the long-term SOC storage in semiarid areas. This study provides a better understanding of temporal changes of SOC to address the restoration of degraded land and adaptation for future trends in global change.

## 1. Introduction

Maintaining SOC stocks is fundamental for supporting long-term agricultural productivity, as well as for mitigating the effects of, and adapting agricultural systems to climate change (Lal, 2015, 2004a; Powlson et al., 2011). Several studies have examined the effects of temperature, precipitation, land use, and geochemistry as drivers of SOC storage (Conant et al., 2011; Hobley et al., 2017; Kirschbaum, 1995; Kramer and Chadwick, 2016; Post and Kwon, 2000). However, these effects are still the focus of many studies as the SOC content is not easy to predictably, mainly because of it is highly dependent on the site characteristics (Chenu et al., 2018; Giardina and Ryan, 2000; Schmidt et al., 2011).

Chile exhibits numerous advantages for studying soil C changes due to a large north-south gradient of climate and geology, and consequently, displays wide variations in SOC stocks and rates of turnover (Bonilla and Johnson, 2012). Arid and semiarid regions comprise 41% of the continental zone (Perez-Quezada et al., 2011), but precipitation ranges widely, from areas with almost no precipitation in the north, up to 3000 mm $yr^{-1}$ in southern Chile (Casanova et al., 2013; Lobo et al., 2015). Due to low vegetation cover and relatively poor soil structure, soils in dry climates are often more prone to SOC depletion because of land degradation and desertification, which is exacerbated by the erosion, salinization of irrigated lands, and the impacts of climate changes (FAO, 2017; Lal, 2004b, 2001). Because of this, during that last several decades we might expect arid and semiarid regions to have relatively greater losses of SOC and associated changes in chemical properties compared to soils under more humid conditions. Conversely, due to

* Corresponding author.
*E-mail address:* cbonilla@ing.puc.cl (C.A. Bonilla).

https://doi.org/10.1016/j.still.2018.10.018
Received 20 June 2018; Received in revised form 14 October 2018; Accepted 19 October 2018
Available online 18 November 2018
0167-1987/ © 2018 Elsevier B.V. All rights reserved.

their low initial SOC content (usually less than 0.5% by weight) and longer SOC residence time, arid and semiarid soils may have considerable potential for C sequestration (FAO, 2004; Farina et al., 2013; Lal, 2009).

The recent advances in Mid-infrared (MidIR) and Near-Infrared (NIR) spectroscopy techniques provide a suitable method to characterize soil chemical composition (Bellon-Maurel and McBratney, 2011; Viscarra Rossel and Behrens, 2010). The infrared spectroscopy technique characterize bands for organic and mineral functional groups including amides, aliphatics, aromatics, and carbonyls, as well as silicate and lattice clay Si—O bonds providing information about soil organic matter (SOM) composition and possible changes in future scenarios (Calderón et al., 2013; Leifeld, 2006; Parikh et al., 2014; Viscarra Rossel et al., 2006). Because of this, MidIR spectroscopy has been typically used to predict diverse soil characteristics through advanced chemometric methods such as partial least squares regression (Leifeld, 2006).

On the other hand, recent studies have focused on the spatial distribution and future changes in SOC stocks in Chilean soils (Bonilla and Vidal, 2011; Minasny et al., 2017; Padarian et al., 2017; Reyes Rojas et al., 2018). The soil descriptions were obtained through soil survey studies performed by the Natural Resources Information Center (CIREN), three or four decades ago. Considering the effects of time, agricultural practices, and climate change, some limitations could be expected in these studies as they do not consider the changes and/or SOC sequestration/loss in recent years. In addition, there is a limited knowledge on the role of the soil of type, climate and land use as drivers for SOC variations in agricultural soils in Chile, and the mechanisms involved in the SOC sequestration. Thus, in this study we compute the SOC losses under contrasting soil types, climates, and land use. SOC changes were evaluated in a series of sites from arid to hyper humid climates, different soil physical and chemical properties, and land use. The main objectives were to: 1) Evaluate and compare SOC losses under different soil types, climate, and agricultural land use over the last decades, 2) identify which agroecosystems have been more affected by SOC losses and, 3) examine the linkage between soil spectral differences and changes in SOC content.

We used a dataset comprised of soils from 51 different sites that were initially sampled between 1968 and 1994 within different soil types and climate conditions across the agricultural lands. These same sites were then sampled again at least 20 years later and characterized in terms of soil physicochemical parameters and spectral differences determined by Fourier-transform MidIR spectroscopy. In addition, this study provides updated information for improving geospatial modeling and SOC projections in Chile or when building SOC global maps.

## 2. Materials and methods

### 2.1. Study site

Sampling sites were located in central Chile, from Valparaíso in the north to the Araucanía Region in the south, which includes most of the cultivated and productive land in the country. The sites extend across a 1000 km transect, from 32 °S to 40 °S in the central valley between the Andes mountains and the coastal range (Fig. 1A). All sites were on slopes of < 6% located at elevations between 30 and 580 m. In general, the climate associated with the sites is characterized by rainfall during the southern hemisphere's winter season (between May to September) and a drier summer season (Fig. 2) (Bonilla and Vidal, 2011). In the arid systems, mean annual temperature (MAT) was about 15 °C, mean annual evapotranspiration (ET) was 1250 mm, and mean annual precipitation (MAP) was 200 mm. In general, sites that received more precipitation also had lower mean annual temperatures. In hyper humid zones, MAT reached 12 °C approximately, with an ET of 750 mm and MAP of 2000 mm.

### 2.2. Soil sampling

The soils were initially sampled in 1968 and later in 1994 for various field surveys conducted by CIREN (CIREN, 2002, 1997a, 1997b, 1996a, 1996b). At that time, sites were georeferenced and local landmarks surrounding the sites were noted. In the second sampling, a total of 51 sites were relocated with GPS and sample in the summers of 2014, 2016, and 2017. In order to evaluate the spatial variability in soil properties, two additional samples were collected in each site in addition to the GPS sampling point. Soils were collected from topsoil horizon described by CIREN and plant residue and O horizon were removed before sampling. Depending on the site, first horizon depths ranged from 8 to 29 cm (Table 1).

### 2.3. Climate data

We classified the CIREN sites according to the aridity regime (UNESCO, 2010), by computing the ratio between MAP and ET (UNEP, 1997, 1992). Continuous monthly temperature and precipitation series from 1980 to 2015 were obtained from stations managed by the Dirección General de Aguas (DGA), Instituto de Investigaciones Agropecuarias (INIA), and Dirección General de Aeronáutica Civil (DGAC). Monthly ET was computed using Hargreaves and Samani (1985) method, after calibrating with ET data from INIA stations.

### 2.4. Land use

The land use and management records were compiled based on interviews with local farmers and satellite imagery interpretation. High-resolution images were obtained from Google Earth Pro, which are available since year 2004. Initially, all sites were used for agricultural purposes, however, some of them changed the land use over the last decades. Some sites were continuously cultivated, while other sites had a short fallow rotation (1–2 years), followed by a period of orchard plantation. According to all these information, sites were classified into three groups based on the land use over the last 10 years: 1) Non-cultivated sites (NC), as those sites abandonment or without agricultural practices, 2) woody perennial (WP) as those sites with forest plantations, vineyards, and orchards, and 3) cultivated sites (C), typically planted with cereal crops and/or vegetables.

In the study, arid, semiarid and subhumid areas are located between 31.0 °S to 35.0 °S. This area is dominated by Mollisols, Inceptisols followed by Alfisols and Entisols (north in Fig. 1B). Intensive agriculture in this region (crops and grazing) began in the 16th century and is largely dependent on irrigation (Ovalle et al., 1999). The humid and hyper humid sites are located in the southern portion of this region (36° to 40 °S), a region where agriculture began to expand at the beginning of the 20th century. Here the Andean foothills are dominated by Andisols with high SOC content (about 110 g C $kg^{-1}$ soil). The cultivated soils are mainly rainfed and largely used for cereal production (Casanova et al., 2013; Rouanet et al., 2005; Valle et al., 2018).

### 2.5. Laboratory and analytical methods

The data for the initial sampling date corresponds to that reported by CIREN and consists of SOC, bulk density, pH, and texture. No archived soil samples exist from the initial CIREN sampling. For the 2014 and 2017 sampling, all soils were air-dried and passed through a 2-mm sieve. As with the initial CIREN survey, the more recent soil samples were analyzed for SOC using the Walkley Black method (Walkley and Black, 1934). The SOC content (g C $kg^{-1}$) in the topsoil horizon were converted into SOC stock (Mg $ha^{-1}$) as follows:

$$SOC_{stock} = BD \times SOC \times D \times 0.1 \quad (1)$$

where, $BD$ = bulk density (g $cm^{-3}$), $SOC$ = SOC content (g C $kg^{-1}$ soil) and $D$ = thickness of the top horizon (cm). The average annual change

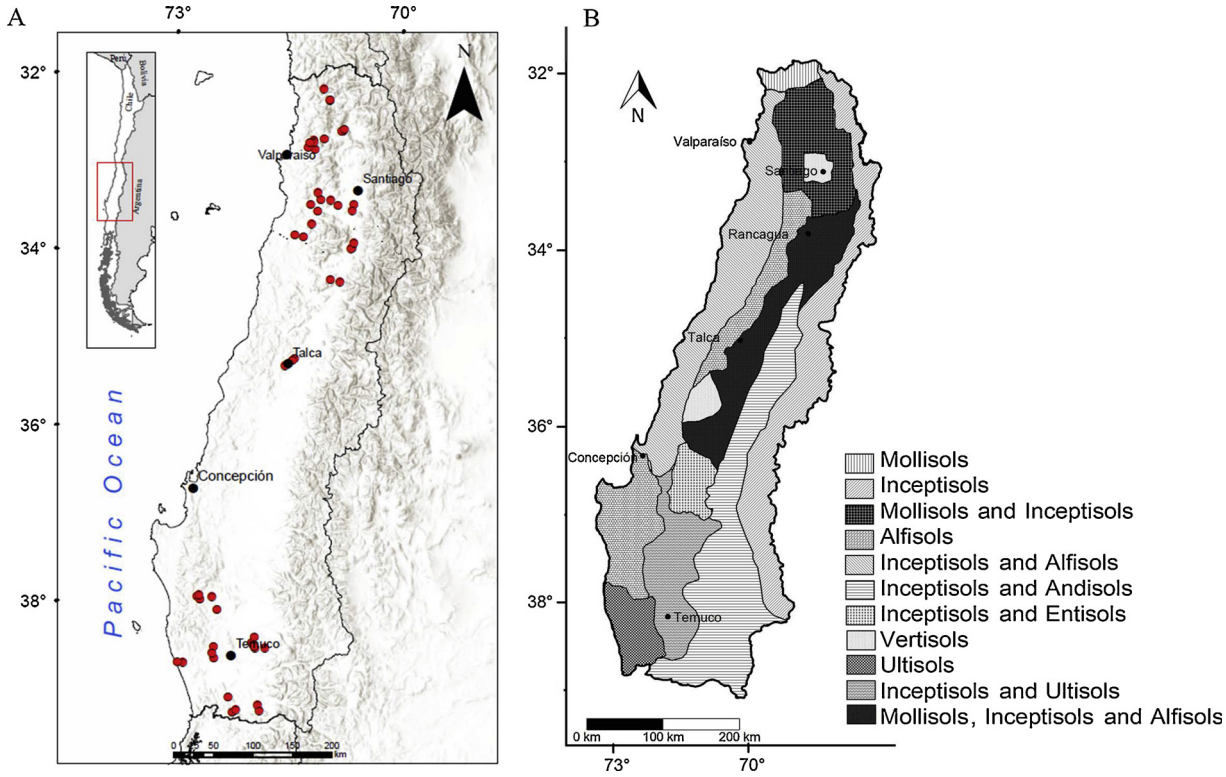


**Fig. 1.** Sampling sites. (A) Sampling sites location in the central Chile, and (B) soil order distribution in the study area (from Bonilla and Johnson, 2012).

rate of SOC stocks ($\Delta CT^{-1}$) (Mg C ha$^{-1}$ yr$^{-1}$), was calculated using the following equation (Zhao et al., 2013):

$$\Delta CT^{-1} = \frac{SOC_{end} - SOC_{ini}}{T_{end} - T_{ini}} \quad (2)$$

where $SOC_{ini}$, $SOC_{end}$ represents the SOC stocks at each sampling period (Mg C ha$^{-1}$). $T_{ini}$, $T_{end}$ represents the initial and final sampling years, respectively.

Soil bulk density (BD) was measured by the core method (Blake and Hartge, 1986). The cores were usually easy to collect without roots and stones in the surface soils of the agricultural plots. Additionally, to ensure the SOC stock were correctly estimated, we collected a minimum of three repetitions per site using cylinders of 5 cm in height and 8.5 cm in diameter, but the BD information was incomplete for 17 of the 51 sites accounting the initial and last sampling. To solve these problems, pedotransfer functions were used to predict BD in those instances (Heuscher et al., 2005). Particle size distribution (clay, silt, sand) was measured by the hydrometer method (Gee and Bauder, 1986). Total N was measured using Kjeldahl digestion and pH was measured in a 1:2.5 soil/water suspension (Sadsawka et al., 2006). Finally, the water-stable aggregates (WSA) were measured using a wet-sieving apparatus (Eijkelkamp, Giesbeek, Netherlands) and calculated as the proportional mass of stable aggregates in the 1–2 mm range relative to the whole soil, as presented by Kemper and Rosenau (1986).

### 2.6. Near-infrared and Mid-infrared spectroscopy

In the absence of archived soils, spectroscopic analysis was only applied to the new soil samples. Prior to scanning with the infrared spectrometer, air-dried soils were dried further at 40 °C, and the dry samples were then ground to a fine powder using a ball mill. These samples were then further homogenized and mixed by hand with an agate mortar and pestle before scanning. All samples were scanned at MidIR (4000 to 400 cm$^{-1}$) and NIR (10,000 to 4000 cm-1) spectral ranges. The NIR has a combination of bands and overtones of spectral bands observable in the MidIR region, which can provide us with unique and complementary information. For example, the NIR is closer to the visible spectrum and can potentially encompass information related to soil color, which is not detected in the MidIR. For this reason, calibrations developed from NIR data often differ in quality from those developed with MidIR absorbances, making it worthwhile to explore calibrations using both spectral ranges. The MidIR does have the advantage that band assignments for specific mineral and organic features are more straightforward than the NIR (Parikh et al., 2014). The MidIR and NIR spectra of the soils were obtained with a Digilab FTS 7000 Fourier-transform spectrometer (Varian, Inc., Palo Alto, CA, now Agilent Technologies) with a Pike AutoDIFF auto-sampler (Pike Technologies, Madison, WI). KBr and Sulfur were used as background samples for the MidIR and NIR, respectively. For the MidIR, a deuterated triglycine sulfate detector and KBr beam splitter were used. A lead selenide detector and a quartz beam splitter were used for the NIR. Each spectrum consisted of 64 co-added scans at 4 cm$^{-1}$ resolution. Spectra were obtained in pseudoabsorbance (log [1/Reflectance]). Two replicate subsamples from each soil were scanned separately and averaged to obtain the spectrum for each CIREN soil. The main spectral bands were selected according to prominent peaks and shoulders observed in the spectra. The assignments for the organic matter and mineral components were carried out using the absorbances reported by Parikh et al. (2014).

### 2.7. Statistical analyses

Correlations between soil properties and climate variables with SOC data were tested for significance using Pearson's correlations in Sigma Plot software. In order to test for significant differences in the percent change in SOC storage between the different soil types and aridity regimes, one-way ANOVA (SigmaStat software) was conducted, with Holm-Sidak multiple comparisons used for testing differences between multiple groups. The data passed a Shapiro-Wilk test for normality and assumptions of homoscedasticity. To determine which site/soil factors

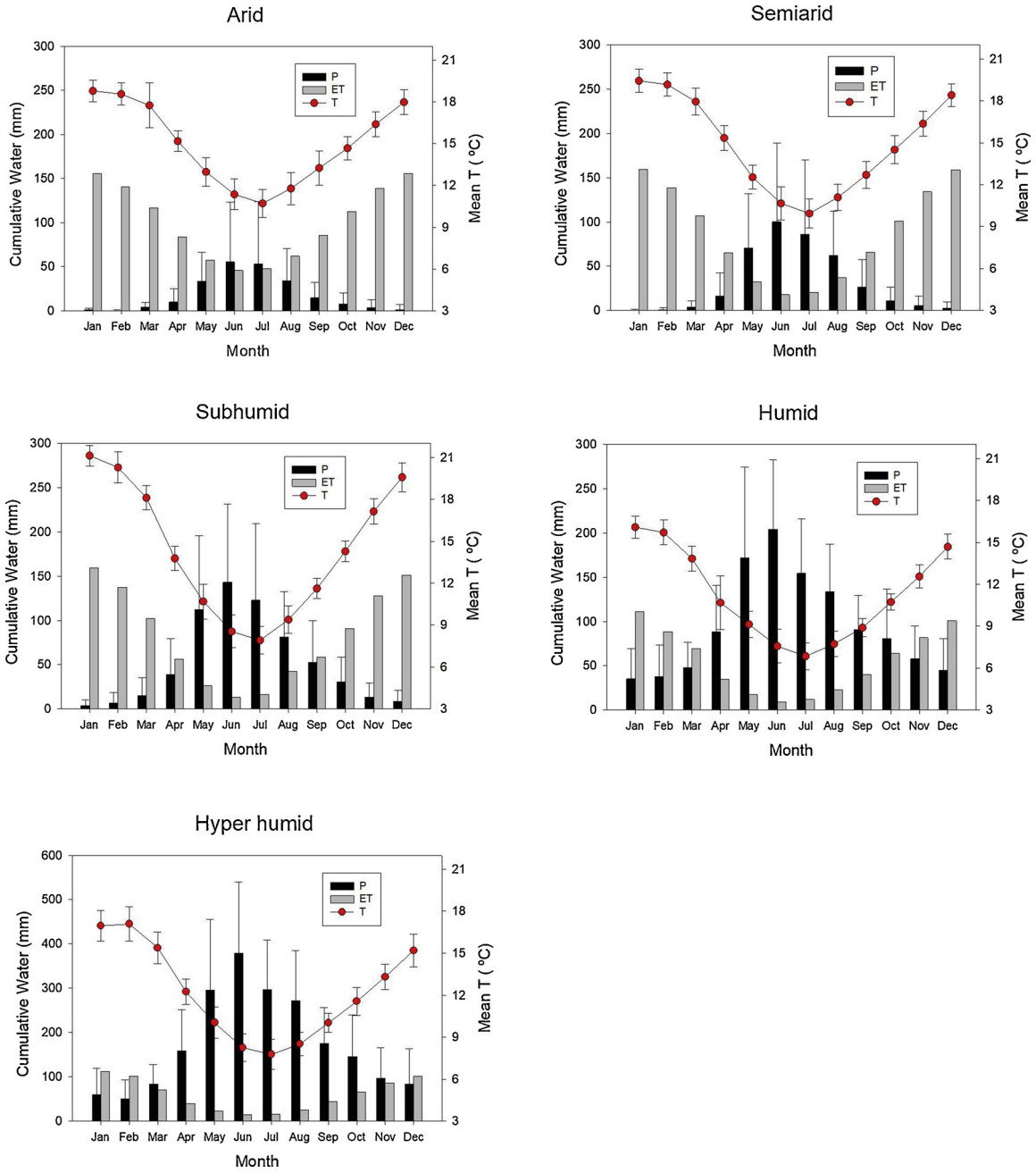


**Fig. 2.** Average monthly of temperature (T), cumulative precipitation (P), and evapotranspiration (ET) in different aridity regimes during the approximate time period considered in this study (1980–2015).

best explained variations in the MidIR and NIR spectral datasets, we performed a Principal Component Analysis (PCA) of all spectra (n = 51) using Unscrambler 10.3 software (Camo Software, Norway). The spectra were mean centered prior to executing the PCA, which included the entire NIR or MidIR spectra. We used the PCA loadings to identify spectral bands that best explained the distribution of sample scores.

Redundancy Analysis (RDA) was performed with Canoco software v5.0 (Microcomputer Power, USA). This was used to visualize the relationships between the nine response variables (rate of change in SOC, and soil physicochemical properties), and the explanatory data set (climate, land use, and soil type). The RDA is a linear, direct gradient ordination method by which the response variables are constrained to be a linear combinations of explanatory variables (ter Braak and Smilauer, 2004). All response variables were centered and standardized before performing the RDA. Interactive forward stepwise selection and Monte Carlo permutation test (499 permutations) were performed to determine the environmental variables influencing the response variables. In the RDA diagrams, arrows that point in the same direction indicate strong positive correlations, while those pointing in opposite directions suggest negative correlations, with arrow length indicating the magnitude of the association.

Chemometric calibrations for WSA (% > 0.25 mm), SOC content (g C $kg^{-1}$ soil) and the difference in SOC contents between sampling times (ΔSOC, g C $kg^{-1}$ soil), were conducted with Partial Least Squares (PLS) regressions using Unscrambler 10.3 (Camo Software, Norway). The spectral data was mean centered, and the validation method was a random cross validation with 20 segments, with 51 calibration samples. The performance of the PLS calibrations and validations were determined by computing the coefficient of determination ($R^2$). When

**Table 1**
Location and main characteristics of the sampling sites.

| Site | Depth (cm) | Latitude (S) | Longitude (W) | Soil order[a] | Aridity regime[b] | Land use | Sampling date |
|---|---|---|---|---|---|---|---|
| 1 | 0-19 | 32.79° | 70.83° | Mollisol | Arid | C | 1979, 2014 |
| 2 | 0-18 | 32.79° | 70.84° | Histosol | Arid | WP | 1979, 2014 |
| 3 | 0-15 | 32.44° | 71.00° | Mollisol | Arid | C | 1979, 2014 |
| 4 | 0-18 | 32.31° | 71.08° | Inceptisol | Arid | WP | 1979, 2014 |
| 5 | 0-23 | 32.43° | 71.00° | Mollisol | Arid | C | 1979, 2014 |
| 6 | 0-16 | 32.77° | 70.81° | Histosol | Arid | NC | 1979, 2014 |
| 7 | 0-18 | 34.12° | 70.73° | Mollisol | Semiarid | WP | 1972, 2014 |
| 8 | 0-8 | 32.99° | 71.21° | Mollisol | Semiarid | C | 1980, 2014 |
| 9 | 0-14 | 33.70° | 71.20° | Mollisol | Semiarid | NC | 1994, 2014 |
| 10 | 0-18 | 34.51° | 70.91° | Alfisol | Semiarid | C | 1972, 2014 |
| 11 | 0-14 | 32.89° | 71.23° | Inceptisol | Semiarid | C | 1994, 2014 |
| 12 | 0-29 | 33.62° | 71.29° | Mollisol | Semiarid | C | 1994, 2014 |
| 13 | 0-16 | 33.84° | 71.28° | Inceptisol | Semiarid | C | 1994, 2017 |
| 14 | 0-22 | 33.96° | 71.52° | Alfisol | Semiarid | NC | 1994, 2017 |
| 15 | 0-14 | 33.98° | 71.40° | Mollisol | Semiarid | WP | 1994, 2017 |
| 16 | 0-23 | 33.49° | 71.19° | Mollisol | Semiarid | C | 1994, 2017 |
| 17 | 0-19 | 33.57° | 71.15° | Mollisol | Semiarid | WP | 1994, 2017 |
| 18 | 0-25 | 33.58° | 71.01° | Mollisol | Semiarid | C | 1994, 2017 |
| 19 | 0-16 | 33.64° | 70.92° | Mollisol | Semiarid | NC | 1981, 2014 |
| 20 | 0-16 | 33.63° | 70.71° | Mollisol | Semiarid | NC | 1981, 2014 |
| 21 | 0-15 | 33.70° | 70.73° | Alfisol | Semiarid | C | 1981, 2014 |
| 22 | 0-17 | 34.48° | 71.04° | Mollisol | Semiarid | C | 1981, 2014 |
| 23 | 0-19 | 34.13° | 70.75° | Mollisol | Semiarid | C | 1983, 2014 |
| 24 | 0-20 | 34.07° | 70.71° | Mollisol | Semiarid | NC | 1983, 2014 |
| 25 | 0-20 | 32.88° | 71.10° | Mollisol | Semiarid | NC | 1980, 2014 |
| 26 | 0-14 | 32.97° | 71.31° | Mollisol | Semiarid | NC | 1980, 2014 |
| 27 | 0-18 | 32.91° | 71.23° | Mollisol | Semiarid | NC | 1994, 2014 |
| 28 | 0-15 | 32.92° | 71.28° | Inceptisol | Semiarid | C | 1994, 2014 |
| 29 | 0-16 | 35.37° | 71.56° | Alfisol | Subhumid | C | 1968, 2017 |
| 30 | 0-23 | 35.45° | 71.70° | Inceptisol | Subhumid | C | 1968, 2017 |
| 31 | 0-15 | 35.39° | 71.60° | Inceptisol | Subhumid | C | 1968, 2017 |
| 32 | 0-20 | 38.04° | 73.06° | Inceptisol | Humid | NC | 1970, 2016 |
| 33 | 0-17 | 38.20° | 72.78° | Alfisol | Humid | C | 1974, 2016 |
| 34 | 0-12 | 38.62° | 72.85° | Inceptisol | Humid | NC | 1974, 2016 |
| 35 | 0-19 | 38.07° | 73.02° | Inceptisol | Humid | C | 1974, 2016 |
| 36 | 0-16 | 38.06° | 72.85° | Inceptisol | Humid | C | 1974, 2016 |
| 37 | 0-16 | 38.02° | 73.03° | Inceptisol | Humid | C | 1974, 2016 |
| 38 | 0-12 | 38.79° | 73.31° | Inceptisol | Hyper humid | NC | 1970, 2016 |
| 39 | 0-12 | 39.31° | 72.24° | Andisol | Hyper humid | NC | 1970, 2016 |
| 40 | 0-17 | 39.38° | 72.62° | Andisol | Hyper humid | WP | 1970, 2016 |
| 41 | 0-10 | 37.93° | 72.69° | Ultisol | Hyper humid | C | 1970, 2016 |
| 42 | 0-16 | 38.66° | 72.11° | Andisol | Hyper humid | C | 1970, 2016 |
| 43 | 0-16 | 38.66° | 72.25° | Andisol | Hyper humid | C | 1970, 2016 |
| 44 | 0-15 | 39.20° | 72.67° | Andisol | Hyper humid | C | 1970, 2016 |
| 45 | 0-16 | 38.60° | 72.30° | Inceptisol | Hyper humid | C | 1970, 2016 |
| 46 | 0-13 | 38.64° | 72.26° | Andisol | Hyper humid | C | 1970, 2016 |
| 47 | 0-17 | 39.35° | 72.57° | Andisol | Hyper humid | C | 1970, 2016 |
| 48 | 0-13 | 38.69° | 72.88° | Inceptisol | Hyper humid | C | 1970, 2016 |
| 49 | 0-20 | 38.77° | 73.39° | Inceptisol | Hyper humid | NC | 1970, 2016 |
| 50 | 0-16 | 38.53° | 72.25° | Inceptisol | Hyper humid | NC | 1970, 2016 |
| 51 | 0-15 | 39.38° | 72.22° | Andisol | Hyper humid | C | 1970, 2016 |

C: Cultivated; NC: Non-cultivated; WP: Woody perennial.
[a] Soil order as reported by CIREN according to Soil Survey Staff (1975).
[b] According to UNESCO, 2010.

**Table 2**
Soil properties of different soils orders samples across a climatic gradient in Central Chile.

| Order (*) | n | Depth (cm) | WSA (% > 0.25 mm) | BD (g $cm^{-3}$) | SOC (g C $kg^{-1}$ soil) | Sand (g 100 $g^{-1}$ soil) | Clay (g 100 $g^{-1}$ soil) | C:N | pH |
|---|---|---|---|---|---|---|---|---|---|
| Andisols | 8 | 15 ± 2 | 86.5 ± 3.0 | 0.6 ± 0.1 | 102.4 ± 22.5 | 44 ± 12 | 14 ± 5 | 18 ± 3 | 5.8 ± 3.2 |
| Alfisols | 5 | 18 ± 2 | 75.6 ± 12.2 | 1.4 ± 0.3 | 17.3 ± 8.9 | 38 ± 11 | 28 ± 5 | 20 ± 4 | 6.5 ± 0.7 |
| Histosol | 2 | 17 | 69.5 | 1.4 | 20.4 | 31 | 30 | 20 | 7.5 |
| Inceptisols | 16 | 16 ± 3 | 81.0 ± 14.8 | 1.2 ± 0.1 | 25.3 ± 11.0 | 45 ± 16 | 22 ± 10 | 16 ± 4 | 6.2 ± 0.9 |
| Mollisols | 19 | 19 ± 5 | 63.0 ± 10.6 | 1.5 ± 0.3 | 15.1 ± 6.2 | 42 ± 18 | 26 ± 9 | 21 ± 7 | 7.5 ± 0.5 |
| Ultisol | 1 | 10 | 92 | 1.1 | 34 | 21 | 45 | 17 | 5.4 |

Values are mean ± standard deviation of the n indicated in the second column. WAS: Water stable aggregates; BD: Bulk density; SOC: Soil organic carbon.

using PLS regression to develop a predictive model, it is important to use the proper number of factors or loading vectors. The first few factors tend to be more related to the soil attributes to be predicted, while the higher number factors tend to increase the model spectral noise. When few factors are included, the accuracy of the PLS model declines because not all the spectral differences related to the constituent are included. Predictive calibrations where a large portion of total variance is explained using a minimal number of factors are desirable. In this study, the optimal number of PLS factors used was determined from the relationship of the explained variance and the number of factors, and this was done automatically by the Unscrambler 10.3 software (Camo Software, Norway). For the MidIR there were 1868 absorbance points used as variables, and five factors were suggested by the model. For the NIR there were 3113 absorbance points used as variables, and five factors were suggested by model.

## 3. Results

### 3.1. Descriptive soil and climate parameters

The average SOC content for the different soil types ranged from 15.1 to 102.4 g C $kg^{-1}$ soil (Table 2). The SOC content, aggregate stability and clay content were high in Andisols with an average 102.4 g C $kg^{-1}$ soil, 86.5% > 0.25 mm, and 14 g 100 $g^{-1}$ soil, respectively. The sites with Mollisols showed the lowest SOC concentrations with an average of 15.1 g C $kg^{-1}$ soil. In general, soil pH ranged from 5.4 to 7.5, with the most acid conditions in the Andisols, and the more alkaline conditions in the Mollisols and Histosols. The C:N ratio varied between 15 and 21, with the lowest values occurring in the Mollisols and Inceptisols. Bulk density had an inverse relationship with SOC, and the Andisols reached the lowest BD values. The SOC concentrations increased from arid to hyper humid conditions (Table 3). In addition, as conditions became more humid, the aggregate stability increased, reaching 88.9% > 0.25 mm in the hyper humid regime. Conversely, bulk density and soil pH were lower in the hyper humid sites, with values of 0.8 g $cm^{-3}$ and 5.8 respectively.

The correlation analysis conducted between climate and soil parameters (Table 5) shows 45 attribute pairs with 12 positive and 15 negative significant ($P < 0.05$) correlated variables. SOC was positive and strongly correlated with MAP (r = 0.88), WSA (r = 0.50) and silt (r = 0.35). Negative correlations were observed between SOC and pH (r = -0.52), MAT (r = -0.68) and BD (r = -0.88). Clay was correlated negatively with SOC content (r = -0.30). However, a significant positive relationship ($P < 0.05$) was observed when SOC and clay contents were grouped into arid-semiarid conditions (r = 0.68). Soil C:N ratio did not vary significantly with SOC content, but showed a significative correlations with WSA (r = -0.53) and MAP (r = -0.31).

The historical meteorological data trends indicated that the mean annual temperatures have slightly increased in subhumid and humid zones by 0.011 and 0.019 °C $yr^{-1}$ respectively, and slightly decreased in hyper humid zones by -0.006 °C $yr^{-1}$ (Table 6). Annual precipitation has generally decreased with time across all sites, but this trend was most pronounced on semiarid, subhumid and hyper humid sites, with rates of change of -4.86, -5.48 and -8.23 mm $yr^{-1}$, respectively.

### 3.2. Carbon storage and climate, soil types and agricultural effects

Table 4 shows the SOC storage changes in the surface horizon between the baseline and most recent samplings. The Mollisols, which decreased by 29.9% with an average SOC loss rate of 0.99 Mg C $yr^{-1}$ were significantly higher than the Inceptisols and Andisols ($P = 0.002$). The average change in SOC storage grouped by aridity regime ranged from 20.4 Mg C $ha^{-1}$ for semiarid to 2.8 Mg C $ha^{-1}$ for hyper humid. Semiarid soils demonstrated a significant decrease ($P = 0.008$) in SOC storage compared to hyper humid areas. Semiarid soils lost 24.7% of their total C stocks with an average change of -0.80 Mg C $yr^{-1}$ during the time period considered, while the subhumid sites lost 26.1% with an average rate of -0.31 Mg C $yr^{-1}$. Soils in arid climates decreased by 8.8% with rate of -0.26 Mg C $yr^{-1}$. Relatively small gains were observed in humid and hyper humid conditions, with increases of 5.4% and 10.5% and average rates of SOC accumulation at 0.04 and 0.06 Mg C $yr^{-1}$, respectively.

The RDA analysis was carried out using the site characteristics, which included aridity regime, land use, and soil properties (Fig. 3). The explanatory variables (climate, land use and soil types) accounted for 54.3% of the total variation. A total of 46.3% of the variation was explained by the first two constrained axes of the RDA, while the first axis explained 38.4% and the second 8.0%. The RDA shows clear differences related to SOC storage and soil physical properties between the dry and humid zones. These differences were explained (P = 0.002) by the soil types and climate conditions. Andisols and Mollisols accounted for 47.5% and 39.2%, respectively. Additionally, hyper humid and semiarid climates accounted for 48.1% and 39.0% of total variation, respectively. Non-significant land use effects were found to explaining the total variation.

Gains in SOC were represented by positive values of annual change rate ($\Delta CT^{-1}$) of SOC stocks, which was positively associated with WSA humid conditions (Fig. 3). Mollisols and Histosols had greater net SOC losses under semiarid/ arid areas, which were represented by an inverse relationship with $\Delta CT^{-1}$. All land use changes types did not seem to affect distinctly the decrease in SOC under semiarid conditions. The negative relationships of $\Delta CT^{-1}$ with pH is explained by the acidity of the Andisols, which prevail on the more humid climates that also tended to accumulate SOC. Soil textural properties such as clay and sand content, and C:N ratio were negatively associated with $\Delta CT^{-1}$.

### 3.3. Spectroscopic analysis

The PCA of the MidIR absorbance data shows that hyper humid samples have different spectral properties compared to soils from the rest of the climate classifications (Fig. 4A). Soils from arid and semiarid regions tend to cluster separately from the humid, subhumid, and hyper humid samples. The Andisols, which generally occur in hyper humid environments, are different from the rest of the soil types. The sample distributions in the PCA analyses are indicative of chemical and mineralogical differences between the soils. PCA loadings are useful

**Table 3**
Mean values for soil properties of different soils across a climatic gradient in Central Chile.

| Aridity regime[a] | n | Depth (cm) | WSA (% > 0.25 mm) | BD (g $cm^{-3}$) | SOC (g C $kg^{-1}$ soil) | Sand (g 100 $g^{-1}$ soil) | Clay (g 100 $g^{-1}$ soil) | C:N | pH |
|---|---|---|---|---|---|---|---|---|---|
| Arid | 6 | 18 ± 3 | 64.0 ± 8.9 | 1.5 ± 0.2 | 14.9 ± 4.6 | 42 ± 16 | 24 ± 8 | 18 ± 3 | 7.7 ± 0.2 |
| Semiarid | 22 | 18 ± 4 | 64.1 ± 11.8 | 1.4 ± 0.3 | 15.7 ± 7.0 | 41 ± 19 | 28 ± 10 | 21 ± 7 | 7.3 ± 0.6 |
| Subhumid | 3 | 18 ± 4 | 73.0 ± 5.1 | 1.3 ± 0.1 | 16.3 ± 3.3 | 32 ± 10 | 27 ± 1 | 18 ± 0 | 6.5 ± 0.1 |
| Humid | 6 | 17 ± 3 | 88.5 ± 8.8 | 1.1 ± 0.1 | 26.5 ± 6.1 | 49 ± 14 | 19 ± 6 | 16 ± 1 | 5.5 ± 0.3 |
| Hyper humid | 14 | 15 ± 3 | 88.9 ± 4.2 | 0.8 ± 0.2 | 73.6 ± 37.9 | 43 ± 12 | 19 ± 10 | 16 ± 5 | 5.8 ± 0.3 |

Values are mean ± standard deviation of the n indicated in the second column. WAS: Water stable aggregates; BD: Bulk density; SOC: Soil organic carbon.
[a] According to UNESCO, 2010.

**Table 4**
Change in soil organic carbon storage and average annual change rate in different soil orders and aridity regime over the last decades.

| Soil order | | | | Aridity regime | | | |
|---|---|---|---|---|---|---|---|
| | Change in SOC storage | | $\Delta CT^{-1}$ | | Change in SOC storage | | $\Delta CT^{-1}$ |
| | (Mg C $ha^{-1}$) | (%) | (Mg C $ha^{-1}$ $yr^{-1}$) | | (Mg C $ha^{-1}$) | (%) | (Mg C $ha^{-1}$ $yr^{-1}$) |
| Andisols | 4.8 (17.8) | 10.3[a] | 0.10 | Arid | −8.9 (36.1) | −8.8[ab] | −0.26 |
| Alfisols | −4.1 (7.8) | −8.23[a] | −0.10 | Semiarid | −20.4 (25.9) | −24.7[b] | −0.80 |
| Histosols | 9.2 | 29.4[a] | 0.26 | Subhumid | −15.1 (9.6) | −26.1[ab] | −0.31 |
| Inceptisols | −1.7 (15.1) | −5.7[a] | −0.05 | Humid | 1.8 (8.9) | 5.4[ab] | 0.04 |
| Mollisols | −26.5 (29.8) | −29.9[b] | 0.99 | Hyper Humid | 2.8 (17.8) | 10.5[a] | 0.06 |
| Ultisols | −1.1 | −3.0[a] | −0.02 | | | | |

SOC: Soil organic carbon; $\Delta CT^{-1}$: Average annual change rate. SOC storage are the mean values calculated from the data of (1972–1994) to (2014–2016). Values in parentheses are the standard deviation. Means not sharing a letter suffix are significantly different according to one-way ANOVA ($P < 0.05$).
[a] Standard deviations and ANOVA results are not provided for the Ultisols and Histosols due to insufficient replication.

because they indicate which spectral bands have more influence over the separation of the samples along each component. Loadings for component 3 indicate that samples from the more humid climates (as well as the high SOC Andisols) have pronounced absorbance at the lattice clay band at 3690 $cm^{-1}$, the aliphatic CH bands between 2930-2850 $cm^{-1}$, and at the 1210 $cm^{-1}$ band assigned to C—O stretch and/or OH deformation (Fig. 4B). Furthermore, component 1 loadings indicate that the Andisols have high absorbance at the broad OH/NH band around 3400 $cm^{-1}$, the aliphatic CH bands between 2930-2850 $cm^{-1}$, the amide I band at 1660 $cm^{-1}$, as well as the polysaccharide C—O—C, C—OH stretch bands at 1140 and 1040 $cm^{-1}$. Conversely, loadings for component 3 indicate that the semiarid soils, which had the highest SOC losses between sampling times, have relatively high absorbance at 2000-1770 (silicates), 1480 (near the band for aliphatic C—H bend), and 1310 $cm^{-1}$ (near the band for ester C—O bend).

A PCA analysis of the MidIR absorbance data from the semiarid soils exclusively shows a separation according to the net change in SOC, indicating that soils that had been susceptible to high C losses also have specific spectral features (Fig. 5A). Component 3 loadings indicate that the arid and semiarid soils that lost the most C were characterized by absorbance at 1200 $cm^{-1}$ (Fig. 5B), attributed to C—O stretch, and/or OH deformation. At the same time, the soils, which had smaller declines in SOC had high absorbance between 1770-2000 $cm^{-1}$, consistent with higher sand Si-O content, and also high absorbance at the lattice clay band at 3700 $cm^{-1}$.

The NIR spectral region contains absorbance related to overtones and combination bands of the MidIR region. Besides that, the NIR also encompasses absorbances close to the visible region. Because of this the NIR is sometimes a useful complement to MidIR data, shedding light on chemical differences between the soil samples beyond those detected with MidIR. The multivariate analysis of the NIR data had similar separations according to climate regime to those obtained with the MidIR data (Fig. 6). The Andisols tended to group together, and completely separate from the Alfisols. However, the NIR absorbance data was not as useful as the MidIR to tell apart the Mollisols samples according to SOC change values (data not shown).

**Table 6**
Linear regression for mean annual temperature and precipitation across different aridity zones from 1980 to 2015.

| Aridity regime | n[a] | MAT[b] (°C) | Rate of change (°C $yr^{-1}$) | MAP[b] (mm) | Rate of change (mm $yr^{-1}$) |
|---|---|---|---|---|---|
| Arid | 6 | 15.2 ± 0.5 | 0.004 | 277 ± 146 | −3.94 |
| Semiarid | 4 | 14.6 ± 0.5 | 0.005 | 436 ± 191 | −4.86 |
| Subhumid | 3 | 14.9 ± 0.4 | 0.011 | 626 ± 227 | −5.48 |
| Humid | 4 | 12.0 ± 0.2 | 0.019 | 1122 ± 226 | −3.84 |
| Hyper humid | 3 | 12.2 ± 0.4 | −0.006 | 1742 ± 368 | −3.23 |

MAT: Mean annual temperature.
MAP: Mean annual precipitation.
[a] Number of meteorological stations used for the analysis.
[b] Standard deviation in 35 years of data.

### 3.4. Chemometric calibrations for WSA, SOC content and ΔSOC

Chemometric calibrations can often be used to predict soil properties using absorbance data. In this study, we set out to determine if NIR and/or MidIR data could be used as an indicator of past change in soil C (as well as other soil properties). Partial least squares regressions were performed in order to develop calibrations for WSA, SOC content and ΔSOC. The calibrations were done with the full NIR or MidIR spectra, with mean centering as the only pre-treatment. The PLS with the MidIR data showed that calibration $R^2$ were moderately good for the prediction of SOC content, but failed to calibrate for ΔSOC and WSA. The MidIR calibration/validation $R^2$ were 0.53/0.47, 0.89/0.60, and 0.55/0.39 for WSA, SOC content, and ΔSOC, respectively. Likewise, the NIR

**Table 5**
Pearson's correlation coefficient (r) among soil and climates attributes used in the study for soil sampled between 2014 and 2016 in central Chile.

| | MAT | WSA | SOC | Sand | Silt | Clay | C:N | pH | BD |
|---|---|---|---|---|---|---|---|---|---|
| MAP | −0.90 | 0.67 | 0.88 | n.s | n.s | −0.44 | n.s | −0.76 | −0.93 |
| MAT | | −0.75 | −0.68 | n.s | n.s | 0.40 | 0.31 | 0.83 | 0.81 |
| WSA | | | 0.50 | n.s | n.s | n.s | −0.53 | −0.79 | −0.60 |
| SOC | | | | n.s | 0.36 | −0.35 | n.s | −0.52 | −0.88 |
| Sand | | | | | −0.80 | −0.78 | n.s | n.s | n.s |
| Silt | | | | | | n.s | n.s | n.s | −0.37 |
| Clay | | | | | | | n.s | 0.35 | 0.43 |
| C:N | | | | | | | | 0.34 | n.s |
| Ph | | | | | | | | | 0.63 |

MAP: Mean annual precipitation (mm); MAT: Mean annual temperature (ºC); WAS: Water stable aggregates (% > 0.25 mm); SOC: Soil organic carbon (g C $kg^{-1}$ soil); BD: Bulk density (g $cm^{-3}$). BD values (17 of 51 soils) computed with pedotransfer functions were excluded from the analysis.
n.s: Non-significant relationship between the two variables, $P > 0.05$.

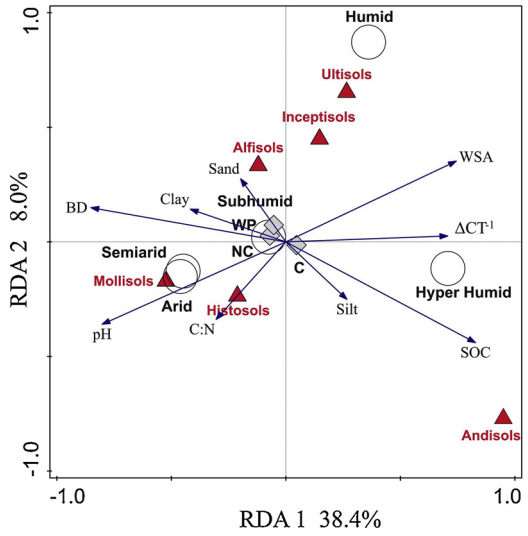


**Fig. 3.** Redundancy analysis (RDA) showing the relationships between SOC content and environmental factors including aridity regime, soil orders and average annual change in SOC ($\Delta CT^{-1}$). Soil order is shown in red triangles, Land uses in gray diamonds and Aridity regimes in white circles. The percent of the variation in the data explained by each axis is shown on the axis label (For interpretation of the references to colour in this figure legend, the reader is referred to the web version of this article).

calibration/validation $R^2$ were 0.40/0.26, 0.73/0.58, and 0.46/0.28 for the WSA, SOC content, and ΔSOC, respectively.

## 4. Discussion

### 4.1. Climate controls on soil C storage

The higher SOC stocks observed under more humid and cooler environments is comparable to previous research showing an increase in SOC with higher latitude in Chilean soils (Bonilla and Johnson, 2012; Padarian et al., 2017). Overall, our field data demonstrates that SOC content has changed over the last decades. Our analyses suggest that climate had a significant influence on soil chemical and physical properties. Furthermore, there is a boundary between the subhumid and humid climates in which the trend for $\Delta CT^{-1}$ reverses, shifting from a net loss of SOC in the drier climates to an increase in SOC in humid and hyper humid areas. High water availability are able to sustain higher primary productivity, and consequently have greater plant residue inputs contributing to a net increase in soil organic matter (Chenu et al., 2018). Hence, the results indicate that climate and initial soil organic carbon content appear to strongly influence SOC stocks, which could accommodate periods of declining precipitation without the moisture becoming a limiting a factor to plant growth and associated C sequestration.

In arid systems, SOC levels may be promoted by the long residence time of SOM as a result of lower soil water availability and lower levels of microbial activity (Austin et al., 2004; Barnard et al., 2013; Stark and Firestone, 1995) and thus may have significant potential for atmospheric C sequestration as (FAO, 2004; Lal, 2009; Stockmann et al., 2013). In general, organic matter decomposition and nutrients release are accelerated in warmer climates, as long as water availability is not a limiting factor (Jobbágy and Jackson, 2000). Here, we found that arid areas have been less impacted by SOC losses compared to semiarid areas. Although these findings may be supported by the fact that agroecosystems in arid region have higher C inputs than natural ecosystems, a meta-analysis performed by Guo and Gifford (2002) evidenced that the effects of land use conversion on soil C stock losses can be strongly influenced by precipitation. For example, after conversion from pasture to crop, areas with 400–500 mm of precipitation lost

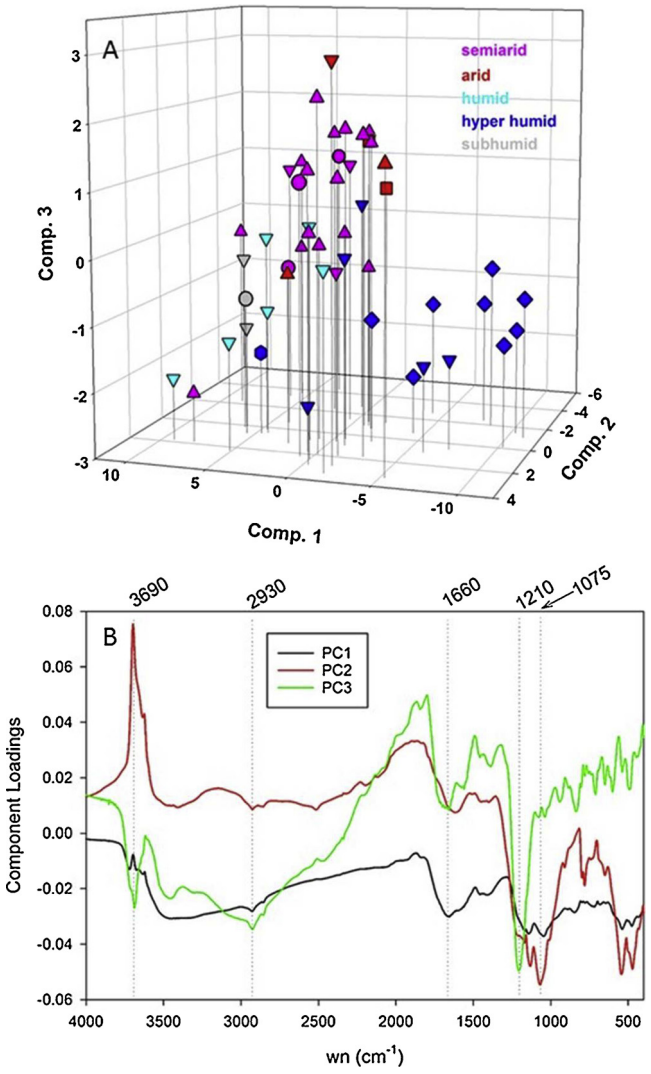


**Fig. 4.** Principal components analysis of the mid infrared spectral data of Chilean soils. Color coded by climate (A). Component 1 explains 75% of the variation, component 2 explains 11% of the variation, and component 3 explains 6% of the variation in the absorbance data. Mollisols are shown in triangles, Alfisols in circles, Inceptisols in downward triangles, Andisols in diamonds, Histosols in squares, and Ultisols in hexagons. Panel (B) shows the component loadings for the principal components analysis shown in (A).

about 75% of the original SOC, and those with 300–400 mm and more than 500 mm, lost 54% and 50%, respectively.

SOC decomposition rates clearly vary with temperature and precipitation but can also be determined by land use and management practices (Bruce et al., 1999; Paustian et al., 2016; Six et al., 1998). Although a non-significant fraction of the variation was accounted for by land use, we cannot simply ignore the effect of land use because it seems to affect the SOC stock differently across climates. We observed that more humid climates exhibited less SOC losses in surface soils compared with drier conditions. Although during the last 20 years the adoption of reduced/non-tillage practices have become more common in southern Chile, conventional tillage is a common practice, which includes the burning of stubble and disk-harrowing operations (Alvear et al., 2005). There is evidence that the effects of tillage on SOC can be relatively minor in moist, cold-temperate soils (Hermle et al., 2008). Furthermore, recent studies have demonstrated that the response of SOC to non-tillage is dependent on climate conditions, in particular precipitation, with a pronounced effect in drier climates (Cosentino et al., 2006; Dimassi et al., 2014).

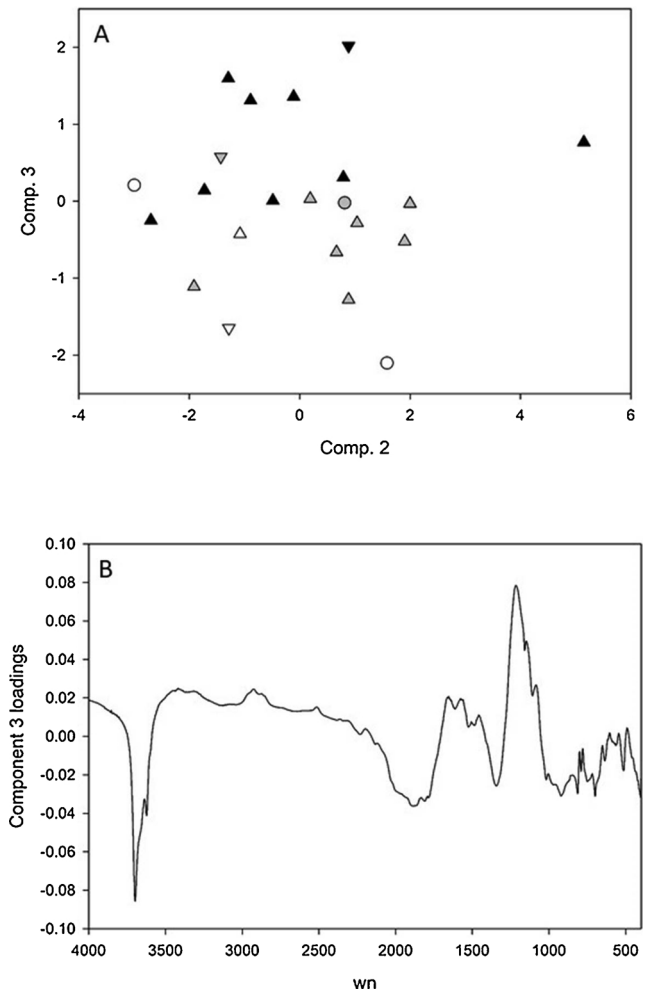


**Fig. 5.** (A) Principal components analysis of the Mid-infrared spectral data from Chilean semiarid soils. Symbol colors are according to SOC change (g C $kg^{-1}$ soil): Black are < -8, grey are between -8 and 0, and white are > 0. Mollisols are shown in triangles, Alfisols in circles, Inceptisols in downward triangles. Component 2 explains 19% of the variation, and component 3 explains 6% of the variation in the absorbance data. (B) Component 3 loadings for the principal components analysis shown in Figure (A).

The abandonment of agricultural lands and subsequent recolonization by natural vegetation is associated with increases in SOC (Novara et al., 2013, 2014,), but our results showed different a trend. Non-cultivated soils do not necessarily increase SOC content compared to cultivated soils in semiarid areas. This is explained by the increasing trend to land abandonment in these areas due to water scarcity, resulting in lower carbon inputs with little or no vegetation. Additionally, soils with woody perennial species were also affected by SOC losses under drier climates. However, it has been shown a soil carbon stock increment in forest soils in deeper soil layers (Lal, 2005), condition that can support the reverse trends observed in arid/semiarid sites. Similarly, a recent study reported that the transition from agriculture to agroforestry land increased by 40% the SOC stock between 0–30 cm depth (De Stefano and Jacobson, 2017).

### 4.2. Soil type controls on soil C storage

The results in this study indicate that soil type was the main factor explaining the soil physicochemical patterns across different areas. The results exhibited similar patterns to previous studies. For instance, Doetterl et al. (2015) found that geochemistry was the most important controlling factor for soil carbon storage in Chilean soils from

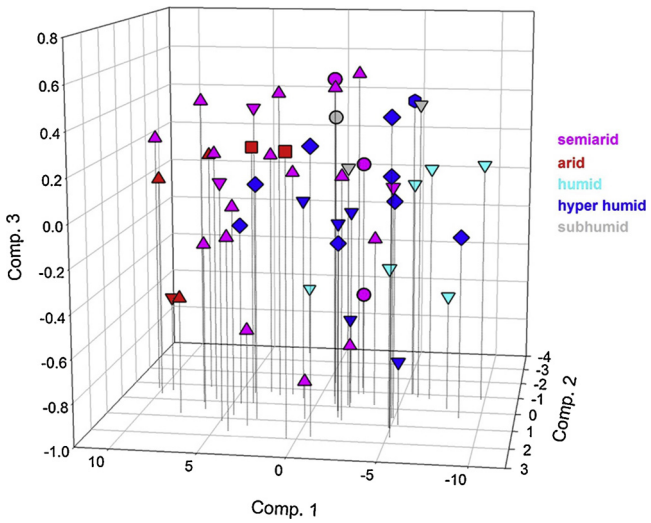


**Fig. 6.** Principal component analysis of the Near-infrared spectral data of Chilean soils color coded by climate. Component 1 explains 95% of the variation, component 2 explains 4% of the variation, and component 3 explains 1% of the variation in the absorbance data. Mollisols are shown in triangles, Alfisols in circles, Inceptisols in downward triangles, Andisols in diamonds, Histosols in squares, and Ultisols in hexagons.

grasslands and shrublands. Additionally, Reyes Rojas et al. (2018) indicated the soil type at suborder level was the best predictor for SOC stock. Arable Mollisols in this study were located in semiarid conditions and were the most prone soil type to SOC losses. In contrast, Andisols, located in more humid areas, had a net increase in SOC during the study period. Mollisols have been considered naturally high in soil fertile and play a significant role as a regional hotspot of carbon (FAO, 2017). However, they are very sensitive to soil degradation and SOC losses (Liu et al., 2012). Similar results have been reported in China, where a loss of 22.3% of SOC has occurred in Mollisols over the past three decades, mainly attributed to high erosion and low input of organic matter (Xu et al., 2017; Yan et al., 2011). Our results confirm that the response of agroecosystems to the temporal SOC variations are site-dependent and site-specific.

### 4.3. Soil physicochemical protection

The RDA analysis indicates that soil aggregate stability tends to be higher in soils that retain SOC, most of them Andisols. These soils, derived from volcanic materials, have been shown to have some of the largest and persistent SOC pools (Huygens et al., 2005; Kramer and Chadwick, 2016). However, Asano and Wagai (2014) demonstrated that the aggregate hierarchy in Andisols is achieved on a micro scale (Oades and Waters, 1991), which limits the comparison of Andisols with other soils in this study. Amorphous inorganic materials, smaller or less-crystalline phyllosilicate clays, and pyrophosphate-soluble metals contribute significantly to Andisols aggregation and organic matter stabilization (Asano and Wagai, 2014; Matus et al., 2014).

Some studies have reported that clay sized minerals tend to be the most important mineral constituents of organo-mineral associations because of their high specific surface area and hydroxylated reactive surfaces (Doetterl et al., 2015). In this study, the clay contents were negatively correlated to SOC content. However, a significant positive relationship was found in arid and semiarid soils, which indicate that physicochemical stabilization mechanisms caused by carbon-clay interactions are predominant in drier areas. This discrepancy across the areas might be related to multiple mechanisms of SOC protection. For instance, the distinctive soil mineralogy in Andisols associated with Al-Fe-Mn oxyhydroxides, as a factor controlling SOC accumulation, is considered to be more relevant than clay content influence (Doetterl

et al., 2015; Matus et al., 2006; Panichini et al., 2017; Takahashi and Dahlgren, 2016).

### 4.4. Use of MidIR to characterize soil the chemical composition

The MidIR spectral properties of soils measured in this study provide insight on their underlying chemical and mineral differences and suggest that samples from different climate regimes and soil types had distinguishing spectral features. Absorbance at 3400 $cm^{-1}$ and 2930-2850 $cm^{-1}$ have been associated with high SOM and C rich fractions in samples from a variety of environments (Calderón et al., 2011a; Matamala et al., 2017). Furthermore, the aliphatic CH absorbance bands between 2930-2850 $cm^{-1}$ have been correlated to permanganate-oxidizable C (POXC), which is a widely used metric of labile soil C (Calderón et al., 2017). Absorbance at 1660 $cm^{-1}$ has been correlated with microbial biomass N (Calderón et al., 2011b), and 1140 and 1040 $cm^{-1}$ have been assigned to labile polysaccharides by others (Parikh et al., 2014). All of these bands had higher absorbance in Andisols, as well as the soils under more humid climates with higher SOC content. This may indicate that the stability of the SOC stocks in Andisols is not due to the inherent recalcitrance of its soil C chemistry, but to other factors such as temperature and mineral protection.

A large body of previous work has demonstrated that it is possible to obtain predictive calibrations for a variety of soil analytes using MidIR and NIR data from diverse soil samples (Parikh et al., 2014). Although our multivariate calibration work shows that spectroscopy and chemometrics hold promise to predict SOC content, predicting past C gains or losses remains elusive. The assumption for this analysis was that there are spectroscopic properties in soils that are related to whether a soil tends to lose or gain SOC over time. Both the NIR and MidIR failed to achieve good calibration quality for aggregation and ΔSOC over time. We suggest a larger set of samples might have been needed to resolve SOC dynamics and soil composition and that spectral characteristics cannot be extrapolated to different soil types, which was consistent with previous studies (Bellon-Maurel and McBratney, 2011; Malley et al., 2004; Stevens et al., 2013).

The spectroscopic data sheds light on the soil characteristics that typify resilient soils. However, it should be noted that these analyses were carried out after the fact, so initial soil characteristics that might have governed SOC protection could have changed since the baseline sampling. Bands associated with soils that lost the most SOC within the arid and semiarid regimes had high absorbance at 1200 $cm^{-1}$. This suggests that moieties that absorb at 1200 $cm^{-1}$ are labile. Oxygen containing functional groups, such as polysaccharide or ether C–O, are preferentially oxidized by soil microbes. As anticipated, clay particles were not associated with SOC retention when all soil types and climates were included in the analysis. However, our spectroscopic results evidence that in semiarid Mollisols, clay protection does have a role in the prevention of SOC losses. Within the arid and semiarid soils (largely Mollisols) lattice clay absorbance at 3700 $cm^{1}$ and quartz(-like) Si-O absorbance at 1770-2000 $cm^{-1}$, was associated with diminished SOC losses. Several studies have shown that layered silicates (also called phyllosilicates) play an important role stabilizing and protecting SOM (Barré et al., 2014; Feng et al., 2013; Six et al., 2002) by adsorption onto phyllosilicate surfaces. Additionally, it has also been reported that charged phyllosilicate clays, and the relatively high SOM content can determine aggregate hierarchy in Mollisols (Asano and Wagai, 2014). In addition, considering the importance of protection and stabilization of SOC, further work is needed to elucidate adsorption mechanisms or physical protection through clay-sized aggregates.

## 5. Conclusions

This research examines the potential effect of climate, soil types and land use on SOC storage under agricultural land. Our findings indicate that SOC content have change over the last three or four decades in agricultural lands, which suggests that these trends must be considered in future studies. The RDA analysis revealed that soil types and climate elicited the most important responses in SOC storage over time. Although, land use does not seem contribute significantly to explain the variance of the soil physicochemical parameter and the rate of SOC changes, the trends show that Mollisols under semiarid conditions in all land use change in our case, are more susceptible to C losses. Additionally, the results indicate that the mechanisms of SOC protection vary with the climate. In semiarid region, our observations suggest that phyllosilicate might play an important role controlling the preservation of SOC. Nevertheless, further studies are needed, given that these soils were not subject to an experimental manipulation, and climate, soil types, and land uses factors are confounded. As Mollisols in semiarid conditions are among the most fertile and productive soils, a better understanding regarding the influence of climate, topography, and management practices would be helpful for future soil restoration efforts.

## Aknowledgements

This research was supported by funding from the National Commission for Scientific and Technological Research, CONICYT/FONDECYT/Regular 1161045. P. Ramírez thanks the support from CONICYT Doctorado Nacional Scholarship 21140873, Government of Chile. The authors also like to extend the thanks to Javier Rivera for his help with the water stability aggregate analysis.

"Disclaimer: The use of trade, firm, or corporation names is for the information and convenience of the reader. Such use does not constitute an official endorsement or approval by the United States Department of Agriculture or the Agricultural Research Service of any product or service to the exclusion of others that may be suitable. The U.S. Department of Agriculture (USDA) prohibits discrimination in all its programs and activities on the basis of race, color, national origin, age, disability, and where applicable, sex, marital status, familial status, parental status, religion, sexual orientation, genetic information, political beliefs, reprisal, or because all or part of an individual's income is derived from any public assistance program."

## References

Alvear, M., Rosas, A., Rouanet, J.L., Borie, F., 2005. Effects of three soil tillage systems on some biological activities in an Ultisol from southern Chile. Soil Tillage Res. 82, 195–202. https://doi.org/10.1016/j.still.2004.06.002.

Asano, M., Wagai, R., 2014. Evidence of aggregate hierarchy at micro- to submicron scales in an allophanic andisol. Geoderma 216, 62–74. https://doi.org/10.1016/j.geoderma.2013.10.005.

Austin, A.T., Yahdjian, L., Stark, J.M., Belnap, J., Porporato, A., Norton, U., Ravetta, D.A., Schaeffer, S.M., 2004. Water pulses and biogeochemical cycles in arid and semiarid ecosystems. Oecologia 141, 221–235. https://doi.org/10.1007/s00442-004-1519-1.

Barnard, R.L., Osborne, C.A., Firestone, M.K., 2013. Responses of soil bacterial and fungal communities to extreme desiccation and rewetting. ISME J. 7, 2229–2241. https://doi.org/10.1038/ismej.2013.104.

Barré, P., Fernandez-Ugalde, O., Virto, I., Velde, B., Chenu, C., 2014. Impact of phyllosilicate mineralogy on organic carbon stabilization in soils: incomplete knowledge and exciting prospects. Geoderma 235, 382–395. https://doi.org/10.1016/j.geoderma.2014.07.029.

Bellon-Maurel, V., McBratney, A., 2011. Near-infrared (NIR) and mid-infrared (MIR) spectroscopic techniques for assessing the amount of carbon stock in soils - Critical review and research perspectives. Soil Biol. Biochem. 43, 1398–1410. https://doi.org/10.1016/j.soilbio.2011.02.019.

Blake, G., Hartge, K.H., 1986. Bulk density., in: methods of soil analysis part 1. Physical and mineralogical methods. Madison 363–375.

Bonilla, C.A., Johnson, O.I., 2012. Soil erodibility mapping and its correlation with soil properties in Central Chile. Geoderma 189–190, 116–123. https://doi.org/10.1016/j.geoderma.2012.05.005.

Bonilla, C.A., Vidal, K.L., 2011. Rainfall erosivity in Central Chile. J. Hydrol. (Amst) 410, 126–133. https://doi.org/10.1016/j.jhydrol.2011.09.022.

Bruce, J.P., Frome, M., Haites, E., Janzen, H., Lal, R., Paustian, K., 1999. Carbon sequestration in soils. J. Soil Water Conserv. 54, 382–389.

Calderón, F., Haddix, M., Conant, R.T., Magrini-Bair, K., Paul, E., 2013. Diffuse-reflectance fourier-transform mid-infrared spectroscopy as a method of characterizing changes in soil organic matter. Soil Sci. Soc. Am. J. 77, 1591–1600. https://doi.org/10.2136/sssaj2013.04.0131.

Calderón, F.J., Culman, S., Six, J., Franzluebbers, A.J., Schipanski, M., Beniston, J., Grandy, S., Kong, A.Y.Y., 2017. Quantification of soil permanganate oxidizable C (POXC) using infrared spectroscopy. Soil Sci. Soc. Am. J. 81, 277. https://doi.org/10.2136/sssaj2016.07.0216.

Calderón, F.J., Mikha, M.M., Vigil, M.F., Nielsen, D.C., Benjamin, J.G., Reeves, J.B., 2011a. Diffuse-reflectance mid-infrared spectral properties of soils under alternative crop rotations in a semi-arid climate. Commun. Soil Sci. Plant Anal. 42, 2143–2159. https://doi.org/10.1080/00103624.2011.596243.

Calderón, F.J., Reeves, J.B., Collins, H.P., Paul, E.A., 2011b. Chemical Differences in Soil Organic Matter Fractions Determined by Diffuse-Reflectance Mid-Infrared Spectroscopy. Soil Sci. Soc. Am. J. 75, 568. https://doi.org/10.2136/sssaj2009.0375.

Casanova, M., Salazar, O., Seguel, O., Luzio, W., 2013. The Soils of Chile. World Soil Book Series. Springer, Dordrecht.

Chenu, C., Angers, D.A., Barré, P., Derrien, D., Arrouays, D., 2018. Increasing organic stocks in agricultural soils: knowledge gaps and potential innovations. Soil Tillage Res In Press, Corrected Proof.

CIREN, 2002. Estudio Agrológico IX Región.Descripciones de suelos, materiales y símbolos. Publicación N°122, Santiago, Chile.

CIREN, 1997a. Estudio Agrológico V Región. Descripciones de suelos, materiales y símbolos. Publicación N°116, Santiago, Chile.

CIREN, 1997b. Estudio Agrológico VII Región. Descripciones de suelos, materiales y símbolos. Publicación N°117, Santiago, Chile.

CIREN, 1996a. Estudio Agrológico VI Región. Descripciones de suelos, materiales y símbolos. Publicación N°114, Santiago, Chile.

CIREN, 1996b. Estudio Agrológico Región Metropolitana. Descripciones de suelos, materiales y símbolos. Publicación N°115, Santiago, Chile.

Conant, R.T., Ryan, M.G., Ågren, G.I., Birge, H.E., Davidson, E.A., Eliasson, P.E., Evans, S.E., Frey, S.D., Giardina, C.P., Hopkins, F.M., Hyvönen, R., Kirschbaum, M.U.F., Lavallee, J.M., Leifeld, J., Parton, W.J., Megan Steinweg, J., Wallenstein, M.D., Martin Wetterstedt, J.Å., Bradford, M.A., 2011. Temperature and soil organic matter decomposition rates - synthesis of current knowledge and a way forward. Glob. Chang. Biol. 17, 3392–3404. https://doi.org/10.1111/j.1365-2486.2011.02496.x.

Cosentino, D., Chenu, C., Le Bissonnais, Y., 2006. Aggregate stability and microbial community dynamics under drying-wetting cycles in a silt loam soil. Soil Biol. Biochem. 38, 2053–2062. https://doi.org/10.1016/j.soilbio.2005.12.022.

De Stefano, A., Jacobson, M.G., 2017. Soil carbon sequestration in agroforestry systems: a meta-analysis. Agrofor. Syst. 92, 285–299. https://doi.org/10.1007/s10457-017-0147-9.

Dimassi, B., Mary, B., Wylleman, R., Labreuche, J., Couture, D., Piraux, F., Cohan, J.P., 2014. Long-term effect of contrasted tillage and crop management on soil carbon dynamics during 41 years. Agric. Ecosyst. Environ. 188, 134–146. https://doi.org/10.1016/j.agee.2014.02.014.

Doetterl, S., Stevens, A., Six, J., Merckx, R., Van Oost, K., Casanova Pinto, M., Casanova-Katny, A., Muñoz, C., Boudin, M., Zagal Venegas, E., Boeckx, P., 2015. Soil carbon storage controlled by interactions between geochemistry and climate. Nat. Geosci. 8, 780–783. https://doi.org/10.1038/ngeo2516.

FAO, 2017. Soil organic carbon: the hidden potential. Faohttps://doi.org/10.1038/nrg2350.

FAO, 2004. Carbon sequestration in dryland soils. World Soil Resources Reports No. 102. Food and Agriculture Organization, Rome.

Farina, R., Coleman, K., Whitmore, A.P., 2013. Modification of the RothC model for simulations of soil organic C dynamics in dryland regions. Geoderma 200–201, 18–30. https://doi.org/10.1016/j.geoderma.2013.01.021.

Feng, W., Plante, A.F., Six, J., 2013. Improving estimates of maximal organic carbon stabilization by fine soil particles. Biogeochemistry 112, 81–93. https://doi.org/10.1007/s10533-011-9679-7.

Gee, G.W., Bauder, J., 1986. Particle-size analysis, in: methods of soil analysis part 1. Physical and Mineralogical Methods. Amer. Soc. Agron. 9, 383–409.

Giardina, C.P., Ryan, M.G., 2000. Evidence that decomposition rates of organic carbon in mineral soil do not vary with temperature. Nature 404, 858–861. https://doi.org/10.1038/35009076.

Guo, L.B., Gifford, R.M., 2002. Soil carbon stocks and land use change: a meta analysis. Glob. Chang. Biol. 8, 345–360. https://doi.org/10.1046/j.1354-1013.2002.00486.x.

Hargreaves, G., Samani, Z., 1985. Reference crop evapotranspiration from temperature. Appl. Eng. Agric. 1 (2), 96–99. https://doi.org/10.13031/2013.26773.

Hermle, S., Anken, T., Leifeld, J., Weisskopf, P., 2008. The effect of the tillage system on soil organic carbon content under moist, cold-temperate conditions. Soil Tillage Res. 98, 94–105. https://doi.org/10.1016/j.still.2007.10.010.

Heuscher, Sa, Brandt, C.C., Jardine, P.M., 2005. Using Soil Physical and Chemical Properties to Estimate Bulk Density. Soil Sci. Soc. Am. J. 69, 51–56. https://doi.org/10.2136/sssaj2005.0051.

Hobley, E., Baldock, J., Hua, Q., Wilson, B., 2017. Land-use contrasts reveal instability of subsoil organic carbon. Glob. Chang. Biol. 23, 955–965. https://doi.org/10.1111/gcb.13379.

Huygens, D., Boeckx, P., Van Cleemput, O., Oyarzún, C., Godoy, R., 2005. Aggregate and soil organic carbon dynamics in South Chilean Andisols. Biogeosciences 2, 159–174. https://doi.org/10.5194/bg-2-159-2005.

Jobbágy, E.G., Jackson, R.B., 2000. The vertical distribution of soil organic carbon and its relation to climate and vegetation. Ecol. Appl. 10 (2), 423–436. https://doi.org/10.1890/1051-0761(2000)010[0423:TVDOSO]2.0.CO;2.

Kemper, W.D., Rosenau, R.C., 1986. Aggregate stability and size distribution. Methods soil anal. Part 1. Phys. Mineral. Methods 9, 425–442. https://doi.org/10.2136/sssabookser5.1.2 ed.c17.

Kirschbaum, M.U.F.F., 1995. The temperature dependence of soil organic matter decomposition, and the effect of global warming on soil organic C storage. Soil Biol. Biochem. 27, 753–760. https://doi.org/10.1016/0038-0717(94)00242-S.

Kramer, M.G., Chadwick, O.A., 2016. Controls on carbon storage and weathering in volcanic soils across a high-elevation climate gradient on Mauna kea, Hawaii. Ecology 97, 2384–2395. https://doi.org/10.1002/ecy.1467.

Lal, R., 2015. Sequestering carbon and increasing productivity by conservation agriculture. J. Soil Water Conserv. 70, 55A–62A. https://doi.org/10.2489/jswc.70.3.55A.

Lal, R., 2009. Sequestering carbon in soils of arid ecosystems. L. Degrad. Dev. 20, 441–454. https://doi.org/10.1002/ldr.934.

Lal, R., 2005. Forest soils and carbon sequestration. For. Ecol. Manage. 220 (1–3), 242–258. https://doi.org/10.1016/j.foreco.2005.08.015.

Lal, R., 2004a. Soil carbon sequestration to mitigate climate change. Geoderma 123, 1–22. https://doi.org/10.1016/j.geoderma.2004.01.032.

Lal, R., 2004b. Carbon sequestration in dryland ecosystems. Environ. Manage. 33. https://doi.org/10.1007/s00267-003-9110-9.

Lal, R., 2001. Potential of desertification control to sequester carbon and mitigate the greenhouse effect. Clim. Change 51, 35–72. https://doi.org/10.1023/A:1017529816140.

Leifeld, J., 2006. Application of diffuse reflectance FT-IR spectroscopy and partial least-squares regression to predict NMR properties of soil organic matter. Eur. J. Soil Sci. 57, 846–857. https://doi.org/10.1111/j.1365-2389.2005.00776.x.

Liu, X., Lee Burras, C., Kravchenko, Y.S., Duran, A., Huffman, T., Morras, H., Studdert, G., Zhang, X., Cruse, R.M., Yuan, X., 2012. Overview of Mollisols in the world: distribution, land use and management. Can. J. Soil Sci. https://doi.org/10.4141/cjss2010-058.

Lobo, G.P., Frankenberger, J.R., Flanagan, D.C., Bonilla, C.A., 2015. Evaluation and improvement of the cligen model for storm and rainfall erosivity generation in central chile. Catena 127, 206–213. https://doi.org/10.1016/j.catena.2015.01.002.

Malley, D.F., Martin, P.D., Ben Dor, E., Roberts, C.A., Workman, J., Reeves Iii, J.B., 2004. Application in analysis of soils. Near-Infrared Spectroscopy in Agriculture.

Matamala, R., Calderón, F.J., Jastrow, J.D., Fan, Z., Hofmann, S.M., Michaelson, G.J., Mishra, U., Ping, C.L., 2017. Influence of site and soil properties on the DRIFT spectra of northern cold-region soils. Geoderma 305, 80–91. https://doi.org/10.1016/j.geoderma.2017.05.014.

Matus, F., Amigo, X., Kristiansen, S.M., 2006. Aluminium stabilization controls organic carbon levels in Chilean volcanic soils. Geoderma 132, 158–168. https://doi.org/10.1016/j.geoderma.2005.05.005.

Matus, F., Rumpel, C., Neculman, R., Panichini, M., Mora, M.L., 2014. Soil carbon storage and stabilisation in andic soils: a review. Catena 120, 102–110. https://doi.org/10.1016/j.catena.2014.04.008.

Minasny, B., Malone, B.P., McBratney, A.B., Angers, D.A., Arrouays, D., Chambers, A., Chaplot, V., Chen, Z.S., Cheng, K., Das, B.S., Field, D.J., Gimona, A., Hedley, C.B., Hong, S.Y., Mandal, B., Marchant, B.P., Martin, M., McConkey, B.G., Mulder, V.L., O'Rourke, S., Richer-de-Forges, A.C., Odeh, I., Padarian, J., Paustian, K., Pan, G., Poggio, L., Savin, I., Stolbovoy, V., Stockmann, U., Sulaeman, Y., Tsui, C.C., Vågen, T.G., van Wesemael, B., Winowiecki, L., 2017. Soil carbon 4 per mille. Geoderma 292, 59–86. https://doi.org/10.1016/j.geoderma.2017.01.002.

Novara, A., Gristina, L., La Mantia, T., Rühl, J., 2013. Carbon dynamics of soil organic matter in bulk soil and aggregate fraction during secondary succession in a Mediterranean environment. Geoderma 193–194, 213–221. https://doi.org/10.1016/j.geoderma.2012.08.036.

Novara, A., La Mantia, T., Rühl, J., Badalucco, L., Kuzyakov, Y., Gristina, L., Laudicina, V.A., 2014. Dynamics of soil organic carbon pools after agricultural abandonment. Geoderma 235–236, 191–198. https://doi.org/10.1016/j.geoderma.2014.07.015.

Oades, J.M., Waters, A.G., 1991. Aggregate hierarchy in soils. Aust. J. Soil Res. 29 (6), 815–828. https://doi.org/10.1071/SR9910815.

Ovalle, C., Aronson, J., Del Pozo, A., Avendano, J., 1999. Restoration and rehabilitation of mixed espinales in central chile: 10-year report and appraisal. Arid Soil Res. Rehabil. 13, 369–381. https://doi.org/10.1080/089030699263258.

Padarian, J., Minasny, B., McBratney, A.B., 2017. Chile and the Chilean soil grid: a contribution to GlobalSoilMap. Geoderma Reg. 9, 17–28. https://doi.org/10.1016/j.geodrs.2016.12.001.

Panichini, M., Neculman, R., Godoy, R., Arancibia-Miranda, N., Matus, F., 2017. Understanding carbon storage in volcanic soils under selectively logged temperate rainforests. Geoderma 302, 76–88. https://doi.org/10.1016/j.geoderma.2017.04.023.

Parikh, S.J., Goyne, K.W., Margenot, A.J., Mukome, F.N.D., Calderón, F.J., 2014. Soil chemical insights provided through vibrational spectroscopy. Adv. Agron. 126, 1–148. https://doi.org/10.1016/B978-0-12-800132-5.00001-8.

Paustian, K., Lehmann, J., Ogle, S., Reay, D., Robertson, G.P., Smith, P., 2016. Climate-smart soils. Nature 532, 49–50. https://doi.org/10.1038/nature17174.

Perez-Quezada, J.F., Delpiano, C.A., Snyder, K.A., Johnson, D.A., Franck, N., 2011. Carbon pools in an arid shrubland in Chile under natural and afforested conditions. J. Arid Environ. 75, 29–37. https://doi.org/10.1016/j.jaridenv.2010.08.003.

Post, W.M., Kwon, K.C., 2000. Soil carbon sequestration and land-use change: processes and potential. Glob. Chang. Biol. 6, 317–327. https://doi.org/10.1046/j.1365-2486.2000.00308.x.

Powlson, D.S., Whitmore, A.P., Goulding, K.W.T., 2011. Soil carbon sequestration to mitigate climate change: A critical re-examination to identify the true and the false. Eur. J. Soil Sci. 62, 42–55. https://doi.org/10.1111/j.1365-2389.2010.01342.x.

Reyes Rojas, L., Adhikari, K., Ventura, S., 2018. Projecting soil organic carbon distribution in central Chile under future climate scenarios. J. Environ. Qual.

Rouanet, J.L., Acevedo, E., Mera, M., Silva, P., Ferrada, S., 2005. In: Rouanet, J.L. (Ed.), Rotaciones de Cultivos y sus Beneficios para la Agricultura del Sur. Fundación Chile, Santiago Chile 91 p. Fund. Chile - Inst. Investig. Agropecu.

Sadsawka, A., Carrasco, M., Grez, R., Mora, M., Flores, H., Neaman, A., 2006. Métodos de análisis recomendados para los suelos de Chile. Ser. Actas INIA 163 N°34.

Schmidt, M.W.I., Torn, M.S., Abiven, S., Dittmar, T., Guggenberger, G., Janssens, I.A., Kleber, M., Kögel-Knabner, I., Lehmann, J., Manning, D.A.C., Nannipieri, P., Rasse, D.P., Weiner, S., Trumbore, S.E., 2011. Persistence of soil organic matter as an ecosystem property. Nature. 478, 49–56. https://doi.org/10.1038/nature10386.

Six, J., Conant, R.T., Paul, E.A., Paustian, K., 2002. Stabilization mechanisms of soil organic matter: implications for C-saturation of soils. Plant Soil 241 (2), 155–176. https://doi.org/10.1023/A:1016125726789.

Six, J., Elliott, E.T., Paustian, K., Doran, J.W., 1998. Aggregation and soil organic matter accumulation in cultivated and native grassland soils. Soil Sci. Soc. Am. J. 62, 1367. https://doi.org/10.2136/sssaj1998.03615995006200050032x.

Stark, J.M., Firestone, M.K., 1995. Mechanisms for soil moisture effects on activity of nitrifying bacteria. Appl. Environ. Microbiol. 61, 218–221.

Stevens, A., Nocita, M., Tóth, G., Montanarella, L., van Wesemael, B., 2013. Prediction of soil organic carbon at the european scale by visible and near InfraRed reflectance spectroscopy. PLoS One 8. https://doi.org/10.1371/journal.pone.0066409.

Stockmann, U., Adams, M.A., Crawford, J.W., Field, D.J., Henakaarchchi, N., Jenkins, M., Minasny, B., McBratney, A.B., V de R. de, Courcelles, Singh, K., Wheeler, I., Abbott, L., Angers, D.A., Baldock, J., Bird, M., Brookes, P.C., Chenu, C., Jastrow, J.D., Lal, R., Lehmann, J., O'Donnell, A.G., Parton, W.J., Whitehead, D., Zimmermann, M., 2013. The knowns, known unknowns and unknowns of sequestration of soil organic carbon. Agric. Ecosyst. Environ. 164, 80–99. https://doi.org/10.1016/j.agee.2012.10.001.

Takahashi, T., Dahlgren, R.A., 2016. Nature, properties and function of aluminum-humus complexes in volcanic soils. Geoderma 263, 110–121. https://doi.org/10.1016/j.geoderma.2015.08.032.

ter Braak, C.J.F., Smilauer, P., 2004. CANOCO For Windows Version 4.53. Plant Research International. Wageningen, The Netherlands. .

UNEP, 1997. World atlas of desertification. United Nations Environment Programme, second. ed. Arnold, London.

UNEP, 1992. World atlas of desertification. United Nations Environment Programme, first. ed. Arnold, London.

UNESCO, 2010. Atlas de Zonas Áridas de América Latina y el Caribe. Dentro del marco del proyecto "Elaboración del Mapa de Zonas Áridas, Semiáridas y Subhúmedas de América Latina y el Caribe". CAZALAC. Documentos Técnicos del PHI-LAC, No25.

Valle, S.R., Dörner, J., Zúñiga, F., Dec, D., 2018. Seasonal dynamics of the physical quality of volcanic ash soils under different land uses in southern Chile. Soil Tillage Res. 182, 25–34. https://doi.org/10.1016/j.still.2018.04.018.

Viscarra Rossel, R.A., Behrens, T., 2010. Using data mining to model and interpret soil diffuse reflectance spectra. Geoderma 158, 46–54. https://doi.org/10.1016/j.geoderma.2009.12.025.

Viscarra Rossel, R.A., Walvoort, D., McBratney, A., Janik, L., Skjemstad, J., 2006. Visible, near infrared, mid infrared or combined diffuse reflectance spectroscopy for simultaneous assessment of various soil properties. Geoderma 131, 59–75. https://doi.org/10.1016/j.geoderma.2005.03.007.

Walkley, A., Black, I.A., 1934. An examination of the Degtjareff method for determining organic carbon in soils: effect of variation in digestion conditions and of inorganic soil constituents. Soil Sci. 63, 251–263. https://doi.org/10.1097/00010694-194704000-00001.

Xu, Y., Chen, Z., Fontaine, S., Wang, W., Luo, J., Fan, J., Ding, W., 2017. Dominant effects of organic carbon chemistry on decomposition dynamics of crop residues in a Mollisol. Soil Biol. Biochem. 115, 221–232. https://doi.org/10.1016/j.soilbio.2017.08.029.

Yan, X., Cai, Z., Wang, S., Smith, P., 2011. Direct measurement of soil organic carbon content change in the croplands of China. Glob. Chang. Biol. 17 (3), 1487–1496. https://doi.org/10.1111/j.1365-2486.2010.02286.x.

Zhao, X., Hu, K., Stahr, K., 2013. Simulation of SOC content and storage under different irrigation, fertilization and tillage conditions using EPIC model in the North China Plain. Soil Tillage Res. 130, 128–135. https://doi.org/10.1016/j.still.2013.02.005.